Applied Catalysis B: Environmental 95 (2010) 408–413

Contents lists available at ScienceDirect

Applied Catalysis B: Environmental

journal homepage: www.elsevier.com/locate/apcatb

A new glass substrate photoelectrocatalytic electrode for efficient visible-light hydrogen production: CdS sensitized TiO_2 nanotube arrays

Jing Bai, Jinhua Li, Yanbiao Liu, Baoxue Zhou *, Weimin Cai

School of Environmental Science and Engineering, Shanghai Jiao Tong University, Shanghai 200240, PR China

ARTICLE INFO

Article history:
Received 7 November 2009
Received in revised form 23 December 2009
Accepted 20 January 2010
Available online 25 January 2010

Keywords:
Transparent
CdS
TiO_2 nanotube arrays
Hydrogen
Glass substrate electrode

ABSTRACT

Transparent and visible-light-response CdS sensitized TiO_2 nanotube arrays (TNAs) photoelectrode was fabricated on conductive glass with the aim to improve the mechanical stability and light utilization of traditional Ti-foil-based titania nanotubes electrode. The sample was studied by FESEM, EDX and XPS to characterize its morphology and chemical compostion. UV–vis absorption spectra and photoelectrochemical measurement approved that the CdS coating enhanced the visible spectrum absorption of the TiO_2 nanotube array, as well as their solar-spectrum induced photocurrents. Under visible-light AM 1.5 illumination (100 mW/cm^2) the composite photoelectrode generate hydrogen from water containing sulfide ions at a rate of 1.12 mL/cm^2 h, nearly 7.46 times higher than that of pure TNAs or 11.79 times than that of commercial P25 glass electrode. Such kind of material will has potential application in solar water splitting and other fields.

1. Introduction

Today, the utilization of solar energy has become a growing interest because of the depletion of fossile resources and the serious environmental pollution made by the fossile combustion [1]. As one of the promising green technologies, solar-hydrogen production from water has attracted much attention in recent years. Generally, this process utilizes a semiconductor material to transfer the solar energy for the production of H_2 from water. Among the semiconducting materials, one of the most used is titanium dioxide (TiO_2) owing to its convenient properties: low cost, relatively high chemical inertia, and high efficiency in photocatalytic processes [2]. Particularly, recent research has been focused on the fabrication of ordered TiO_2 nanotube arrays (TNAs) due to their superior performance over TiO_2 nanoparticles [3–7]. The microstructure of the nanotube at length and pore size can be conveniently controlled by the anodization parameters including electrolyte composition, voltage and duration. Furthermore, when a positive bias potential is applied across the TiO_2 film, it becomes more favorable for photoelectrons to transfer into the external circuit hence effective separation of photohole/photoelectrons pairs; therefore, they have great potential to harvest sunlight and use the photoelectrons efficiently to generate H_2 [8,9].

A critical drawback of titania, however, is that it is a large gap semiconductor (E_g = 3.2 eV), which can only be excited by UV radiation with wavelength below 380 nm. This factor strongly limits the absorption of sunlight to the ultraviolet region of the solar spectrum, therefore, it is ineffective for the utilization of solar energy by pure TiO_2 nanotube arrays. To improve the sunlight photocatalytic efficiency, many promising studies were attempted to dope TiO_2 with non-metals [10–12], or coupling it with a low band gap semiconductor material [13–15]. CdS is considered to be an important sensitizer used for large band gap semiconductors since it has a narrow band gap (2.4 eV) and its conduction band level is slightly higher than that of TiO_2 [16,17]. Hence, as a kind of photosensitive materials, CdS can induce an efficient and longer charge separation by minimizing the electron–hole recombination in TiO_2. To date, the CdS have been decorated on the Ti-based TNAs electrodes by different methods, such as electrochemical deposition [18–22] and sequential-chemcial bath deposition (S-CBD) [23–27], and as reported, the existence of CdS greatly enhanced the photoactivity of TNAs under the visible-light illumination.

However, the combination between nano-TiO_2 film and the substrate directly influencing the electrons transfer performance of the electrode materials. Although the Ti-based titania nanotubes has several advantages as described above, their susceptibility to mechanical shock/vibrations limits the application of this material architecture. It is common for nanotubes, especially for long nanotubes, to tilt, rupture or even peel off the surface of the substrate when a mechanical force is applied to the surface of the film [28]. Moreover, the opaque Ti metal substrate also completely

* Corresponding author. Tel.: +86 21 54747351; fax: +86 21 54747351.
E-mail address: zhoubaoxue@sjtu.edu.cn (B. Zhou).

0926-3373/$ – see front matter © 2010 Elsevier B.V. All rights reserved.
doi:10.1016/j.apcatb.2010.01.020

blocks the light coming through, which restricts light utilization. Therefore, to fabricate a layer of titania nanotubes on a transparent glass will be very promising for various applications including solar water splitting, dye-sensitized solar cells [29], and environmental pollution treatment, since it can overcome the change of internal stress caused by the external mechanical force and favor light utilization. However, to the best of our knowledge, there has been no study to date regarding such CdS sensitized glass-based TiO_2 nanotubes electrode applied into solar water splitting.

In our previous work, we have reported the preparation of Ti-based TiO_2 nanotube arrays or nanopore arrays with different morphological characteristics, and applied them as photoanodes in photoelectrochemical applications such as water splitting, organic pollutant degradation and COD determination etc [5–7,30–32]. In this study, a new glass substrate photoelectrocatalytic electrode of CdS sensitized TiO_2 nanotube arrays for efficient visible-light hydrogen production was prepared by using a chemical bath deposition method [27]. The morphologies, chemical compostion and photoelectronchemical property of the obtained CdS/TNAs were characterized, respectively. At last, the efficiency for photocatalytic hydrogen generation was examined.

2. Experimental

2.1. Preparation of S-CBD synthesized CdS/TNAs glass electrode

For experiment, the FTO glass (Asahi Glass Fabritech Co., Ltd.) is rinsed in deionized water, followed by heating to 250 °C for removing the H_2O molecule on the surface and finally cooling down to room temperature in air. After that, a thickness of 1 μm Ti film was spattered on the glass by 1 μm/h, using a spatter device working in 3.2×10^{-3} Torr air pressure with protection gas of argon (Ar). The morphology of sputtered Ti film was characterized (see the supporting information, Fig. S1(a)). In a typical fabrication process, the titanium film was cleaned with acetone in an ultrasonic bath, followed by rinsing in deionized water and finally drying in air. The TNAs were grown by potentiostatic anodization at 30 V for 1 h in Ethylene Glycol solution containing 0.30 wt% NH_4F and 2.0 vol% deionized water. Then the resulting electrodes were annealed at 500 °C for 2 h in the air atmosphere.

CdS nanoparticles were deposited into the crystallized TiO_2 nanotubes by S-CBD method [27]. The electrode was immersed into $CdSO_4$ solution and Na_2S solution, respectively, as one cycle for several times until the surface became deep yellow. Finally, the as-prepared samples were dried in a N_2 stream.

For the control experiment, TiO_2 NPs (TNPs) glass electrode was prepared by coating the commercial P25 on conductive glass using the screen-printing method [33]. The electrode after P25 coating is dried in an air oven (150 °C) overnight, followed by annealing in air atmosphere for 3 h at 500 °C. The CdS/TNPs glass electrode was also prepared by the same method (S-CBD).

2.2. Characterization of the prepared samples

The glass electrode morphology was characterized using field emission scanning electron microscopy (FESEM FEI-Sirion200). Energy dispersive X-ray (EDX) analysis is obtained using an Oxford detector. The elements present in the glass electrode were identified by X-ray photoelectron spectroscopy (XPS, VG Microlab 310F, Al Kα radiation). UV–visible absorption spectra of the samples were recorded on a photospectrometer (TU-1901, Pgeneral, China).

All photoelectrochemical measurements and applications are conducted in a quartz cell with a three-electrode configuration composed of the nanotube or TNPs photoelectrode (with an area of 1 cm^2) as a working electrode, Pt foil cathode as a counter electrode, and an Ag/AgCl as a reference electrode. An external Xenon lamp with an AM 1.5 filter (a radiation intensity of 100 mW/cm^2) is used as light source and 1 mol/L sodium sulfide (Na_2S) as the electrolyte solution. The working electrode potential and current are controlled by an electrochemical workstation (CHI 660c, CH Instruments Inc. USA). The amounts of H_2 evolved were gathered and then analyzed by gas chromatography (PE, USA, AutoSystem XL GC).

3. Results and discussion

Fig. 1 shows the visual image of CdS/TNAs glass electrode. It can be seen that the TNAs electrode can be transparent after anodization process that is able to fully transform a thin Ti metal layer on a conductive glass into a TiO_2 nanotubular array. In order to investigate the microstructure of the transparent film, illustrative top and cross-sectional FESEM images of the TiO_2 nanotube arrays used in this work before (Fig. 2a and c) and after the decoration with CdS nanoparticles (Fig. 2b and d) are shown in Fig. 2. The nanotubes observed in Fig. 2a and c have a length of ~900 nm, and a barrier layer thickness of ~20 nm; the average pore diameter as calculated from the FESEM images was 83 ± 3 nm and wall thickness of 10 ± 2 nm. Since the TiO_2 nanotube arrays were successfully synthesized from the Ti film, CdS can be deposited on the TiO_2 nanotube arrays to fabricate CdS/TiO_2 nanotube arrays. It can be seen from Fig. 2b and d that most of the surface area shows open and nicely decorated tubes where individual CdS nanoparticles have a diameter of ~10 nm.

Fig. 3 shows the energy dispersive X-ray investigations carried out with the surface of the decorated TNAs glass electrode. The elemental composition of CdS/TNAs film has been analyzed and the characteristic elements were identified using an EDX detection spectrometer. The area with CdS/TNAs film shows that strong Kα and Kβ peaks from Ti element appear at 4.51 and 4.92 keV, while a moderate Kα peak of the element O appears at 0.52 keV. Besides all the above peaks, elements S, Cd and Sn can also be found (see spectrum 1). Oppositely, the main elements on the area without CdS/TNAs film only are Si, O and Sn, applying the composition of glass/FTO substrate (see spectrum 2).

In order to further investigate the chemical compostion and oxidation state of CdS on the decoated and anealed nanotubes, XPS measurements were performed. Fig. 4a shows a typical XPS survey scan for the CdS/TNAs composite material over a large energy range at low resolution, which represents Ti,Cd, S, O and some traces of carbon. Fig. 4b shows the high resolution XPS spectra of

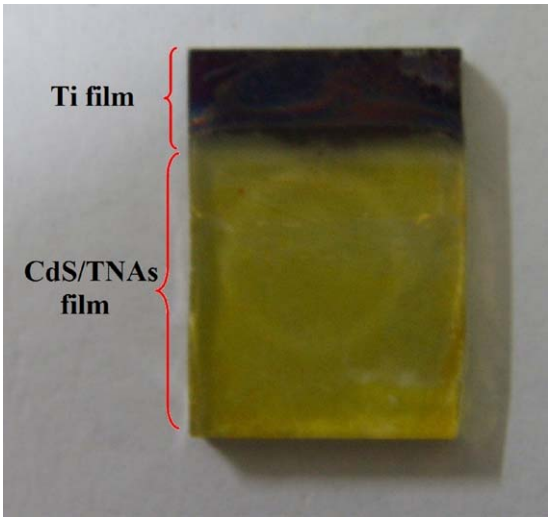

Fig. 1. The visual image of CdS/TNAs glass electrode.

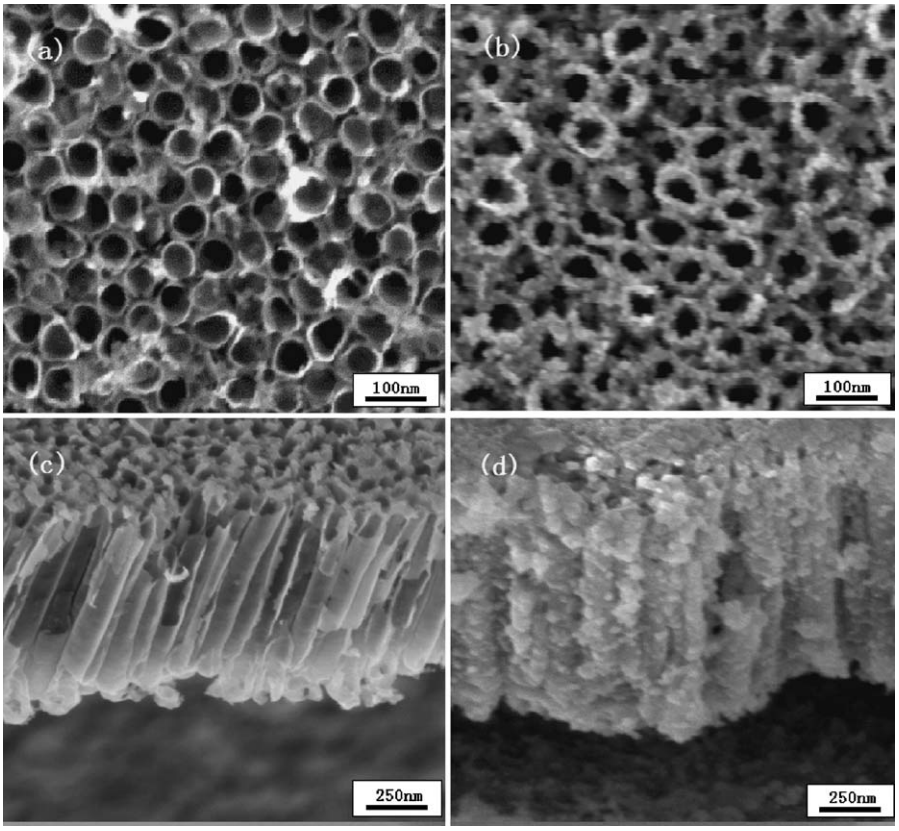

Fig. 2. FESEM images of TNAs films: (a) top view and (c) cross-section of pure TNAs, (b) top view and (d) cross-section of CdS/TNAs.

the CdS peak with $Cd3d_{5/2}$ and $Cd3d_{3/2}$ at 405.2 eV and 411.9 eV, which can be assigned to Cd^{2+} of CdS particles. The S2p peak was observed at 161.8 eV (see Fig. 4c), corresponding to $S^{2-}$of CdS nanoparticles. These results further confirm that the obtained samples are composed of CdS and TiO_2.

Fig. 5 shows the UV–vis absorption spectra of pure TNAs glass electrode and coupled CdS/TNAs glass electrode. It can be seen that pure TNAs absorbed in the UV region with a band edge ~361 nm, on the other hand, the absorption edge of CdS/TNAs composite falls into the visible region at the wavelength of 541 nm as similar as that previously reported [24,34] and it is red-shifted about 180 nm in comparison with that of pure TNAs demonstrating that the absorption spectrum of TNAs can be sensitized with CdS nanoparticles.

The photoelectrochemical properties of the resulting electrodes were tested in a standard three-electrode assembly, which consists of the TNAs or TNPs electrode as a working electrode, Pt foil as a counter electrode, Ag/AgCl as a reference electrode, and 1 mol/L sodium sulfide (Na_2S) as an electrolyte solution. The working electrode was illuminated with AM 1.5 solar light as a voltage sweep from −1.40 to 0.20 V vs Ag/AgCl with a sweep rate of 5 mV/s.

Fig. 6 shows the photocurrent density generated from the pure TNAs and CdS/TNAs glass electrode as well as TNPs glass electrode. It is obvious that a maximum photocurrent density of 4.80 mA/cm^2 is obtained for the CdS/TNAs, while only 0.75 mA/cm^2 was obtained by pure TNAs. It indicates that CdS sheath can be used to sensitize the TNAs and make them more responsible to the visible spectrum. Compared with TNAs electrode, the TNPs

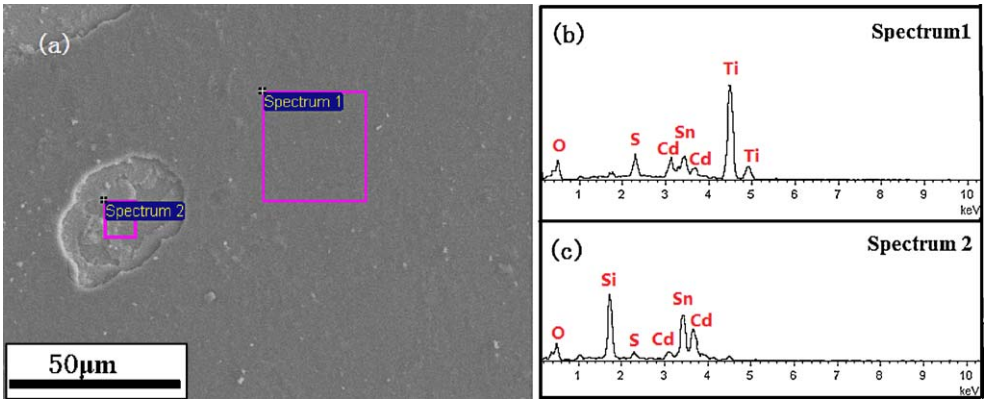

Fig. 3. Energy dispersive X-ray (EDX) spectrum of the CdS/TNAs glass electrode: (a) FESEM surface images of electrode, (b) EDX spectrum of CdS/TNAs film, (c) EDX spectrum of glass/FTO substrate.

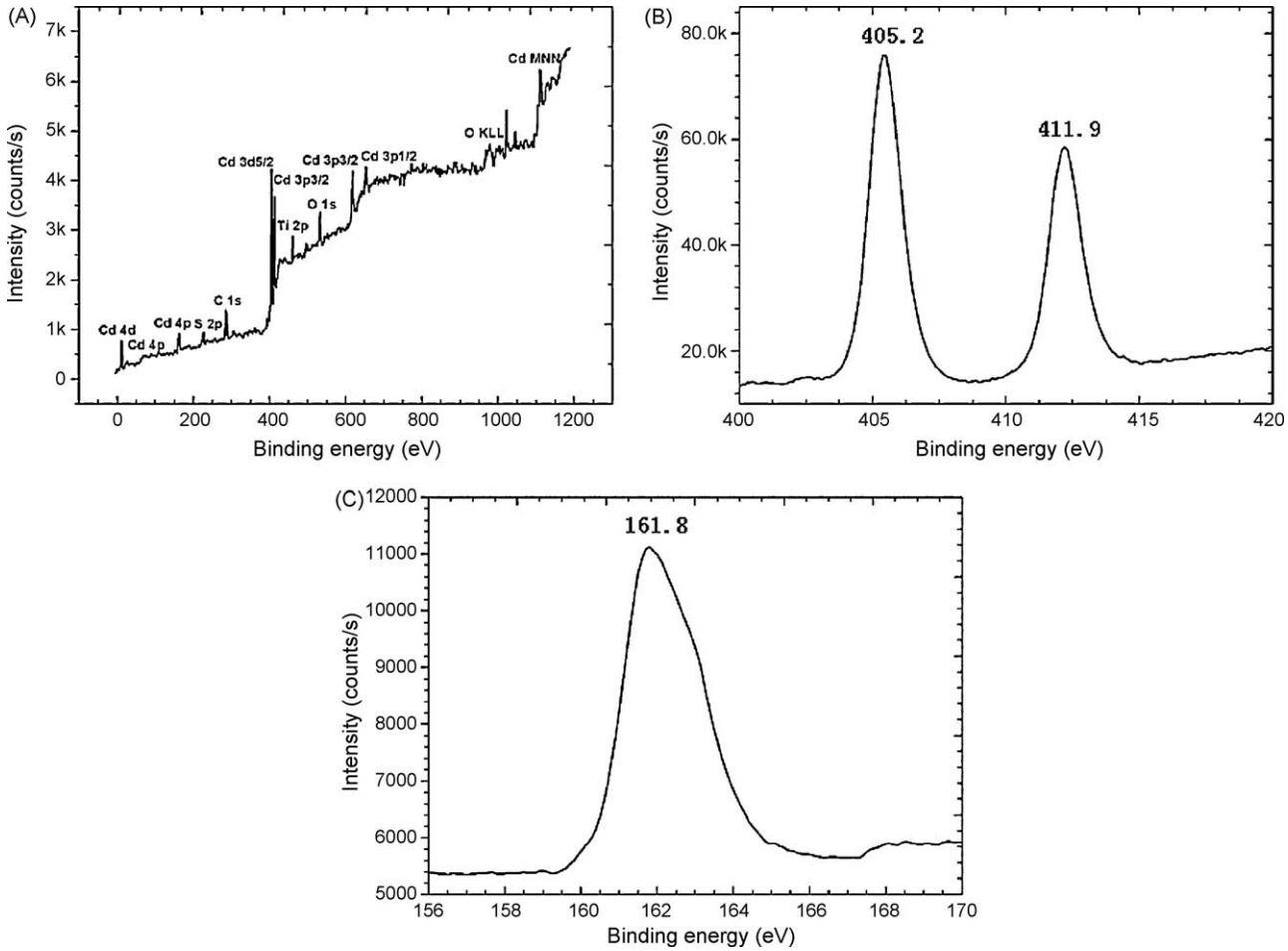

Fig. 4. (a) X-ray photoelectron spectroscopy survey scan over a large energy range at low resolution and high resolution Cd 3d (b), S2p (c) XPS spectra for CdS/TNAs glass electrode.

electrode shows much lower activity whether or not CdS QDs were deposited on it. Their photoconversion efficiencies (η) were calculated as follows [10].

$$\eta(\%) = \frac{(\text{total power output} - \text{electrical power output})}{\text{light power input}} \times 100$$
$$= j_p[(1.23 - |E_{app}|)/I_0] \times 100$$

where j_p is the photocurrent density (mA/cm^2), $j_p|E_{app}|$ the electrical power input and I_0 the power density of incident light (mW/cm^2). The applied potential $E_{app} = E_{mea} - E_{aoc}$ where E_{mea} is the electrode potential (vs Ag/AgCl) of the working electrode at which photocurrent was measured under illumination and E_{aoc} is the electrode potential (vs Ag/AgCl) of the same working electrode at open circuit conditions under same illumination and in the same

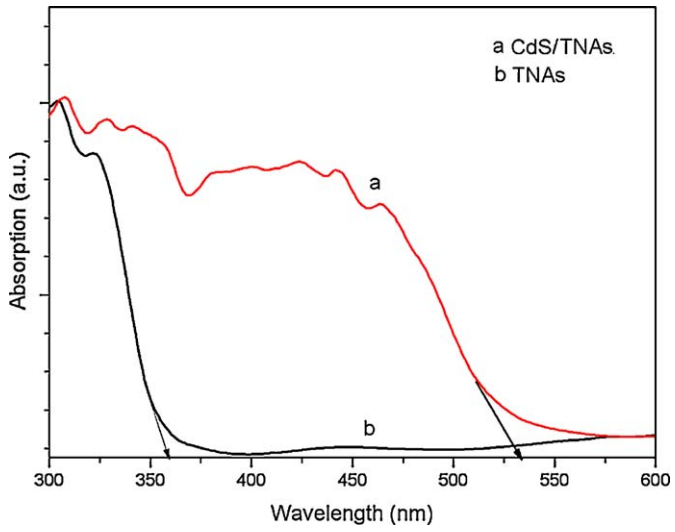

Fig. 5. Absorption spectra of (a) CdS/TNAs and (b) pure TNAs glass electrode.

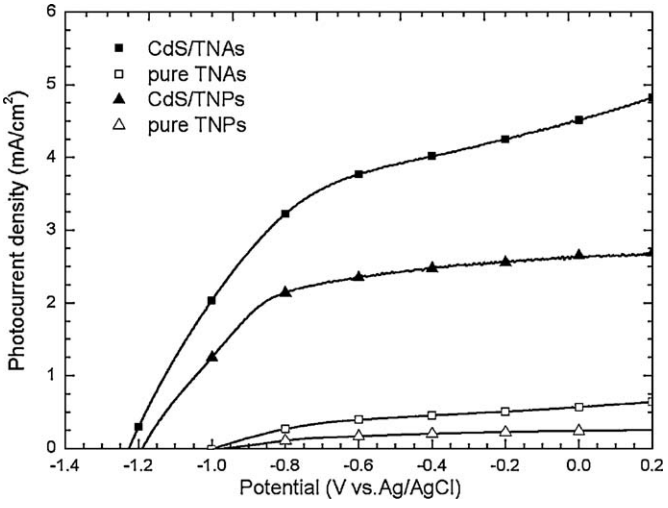

Fig. 6. Photocurrent density vs applied potential for the CdS modified TNAs (■) and TNPs (▲) glass electrode; pure (□) TNAs and TNPs (△) glass electrode illuminated under AM 1.5 visible-light (100 mW/cm^2) illuminations.

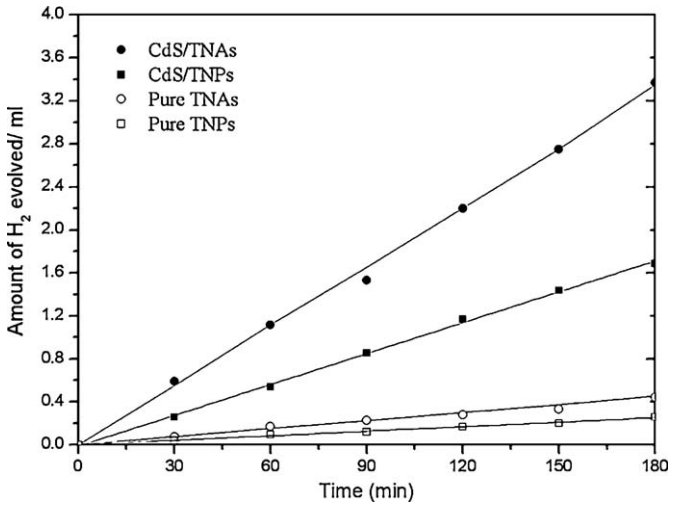

Fig. 7. The rate of hydrogen generation from (a) CdS/TNAs and (b) pure TNAs glass electrode.

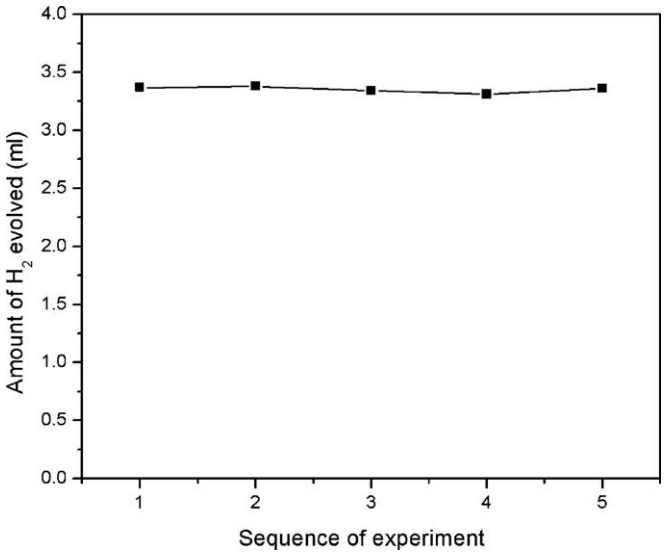

Fig. 8. Stability of CdS/TNAs electrode for generating H_2 in 3 h during a series of 5 identical tests.

electrolyte. A maximum conversion efficiency of 2.58% is achieved for CdS/TNAs whereas the pure TNAs only have a conversion efficiency of 0.33%.

Fig. 7 shows the hydrogen generated as a function of time using pure TNAs and CdS/TNAs glass electrode as well as pure TNPs and CdS/TNPs electrode, respectively. The bias potential was chose at −0.60 V. By measuring hydrogen evolved at each photoanode, the corresponding hydrogen rate is 0.15 ml/cm^2 h for pure TNAs and 1.12 ml/cm^2 h for CdS/TNAs glass electrode; correspondingly it is only 0.095 ml/cm^2 h for pure TNPs and 0.54 ml/cm^2 h for CdS/TNPs glass electrode. These show that the quantity of H_2 produced by CdS/TNAs glass electrode is nearly 7.46 times higher than that of pure TNAs or 11.79 times than that of commercial P25 glass electrode.

The stability of CdS/TNAs was also estimated. Fig. 8 shows the quantity of H_2 produced by CdS/TNAs glass electrode in 3 h during a series of 5 identical tests. As can be seen from Fig. 8, the quantity of generated H_2 was rather stable with an average evolved rate of 3.35 ± 0.03 ml/cm^2. The stability was also approved by comparing the morphology of used CdS/TNAs with that of fresh sample (See the supporting information, Fig. S2). These results indicate that CdS/TNAs glass electrode processes good stability and reliability to generate H_2 for a long period of time.

The mechanism of the Ti-based CdS/TNAs has been explored in some works [21–23], as reported, difference in the positions of conduction bands drives photoelectrons generated in CdS upon initial light absorption to surrounding TiO_2. Moreover, the tubular structure is useful for separating and directing electrons to the collecting electrode surface. In this case, the composite offered remarkable photoconventional efficiency. Herein electron transfer in the CdS/TNAs glass electrode was proposed in Fig. 9 as below:

In aqueous solution, Na_2S in water forms hydroxide (OH^-) and hydrogen sulfide (HS^-) (Eq. (0)). Under light irradiation, CdS is excited and the photogenerated electrons transfer from the conduction band of CdS into TiO_2 and accumulate in the lower-lying conduction band of TiO_2, while the photogenerated holes accumulate in the valence band of CdS (Eqs. (1) and (2)). Since the photoelectrode and Pt counter electrode constitute a circuit, under the light illumination, the applied bias potential drives the electron transfers from TiO_2 nanotube to barrier layer and then to conductive substrate (Eq. (3)) and ultimately to Pt foil (Eq. (4)). Consequently, the photogenerated electrons are scavenged by hydrogen ion on the Pt foil, forming hydrogen gas (Eq. (5)), while the photogenerated holes oxidize S^- to S_2^- on surface of CdS/TiO_2 nanotube (Eq. (6)). This results in a good separation of electron and hole corresponding to much higher photoconversion efficiency. The major reactions that occur in this system can be summarized as follows:

$$H_2O + Na_2S \rightarrow (Na^+OH^-) + (Na^+HS^-) \quad (0)$$

$$CdS + h\nu \rightarrow CdS(h^+, e^-) \quad (1)$$

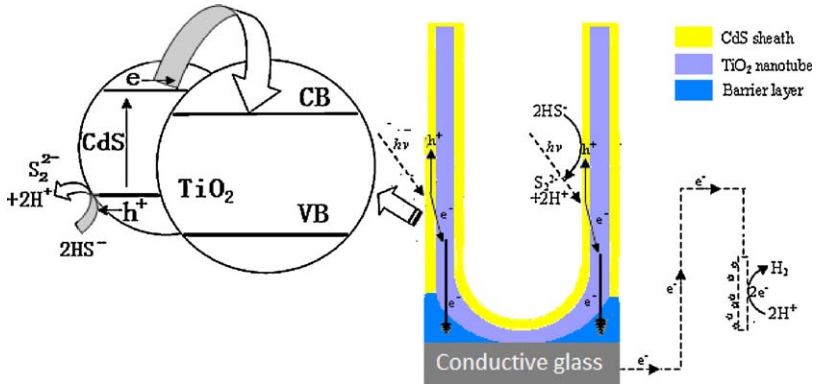

Fig. 9. A configuration model consisting of CdS/TNAs glass electrode and Pt cathode for hydrogen generation.

$$CdS(h^+, e^-) + TiO_2 \rightarrow CdS(h^+) + TiO_2(e^-) \quad (2)$$

$$TiO_2(e^-) \rightarrow TiO_2 + Glass/FTO(e^-) \quad (3)$$

$$Glass/FTO(e^-) \xrightarrow{Pt} Pt(e^-) + Glass/FTO \quad (4)$$

$$Pt(e^-) + 2H^+ \rightarrow Pt + H_2 \quad (5)$$

$$CdS(h^+) + 2HS^- \rightarrow CdS + S_2^{2-} + 2H^+ \quad (6)$$

4. Conclusion

Transparent and well-aligned TiO_2 nanotube arrays (TNAs) on glass substrate, with tube length of ~900 nm and a pore diameter of 83 ± 3 nm, was obtained by anodization of sputtered Ti foil on transparent glass substrate with the aim to improve the mechanical stability and light utilization of traditional Ti-foil-based titania nanotubes electrode, and then CdS was deposited on its surface using chemical bath deposition method for solar-hydrogen production from water. The experimental results indicate that the CdS sensitized glass-based TiO_2 nanotubes electrode shows an efficient charge separation, caused by fast diffusion of photoelectrons generated from CdS toward TiO_2, leading to high photocatalytic activity of hydrogen production. At last, a schematic diagram to describe the mechanism of CdS sensitized TNAs electrode for hydrogen production was proposed.

Acknowledgements

The authors would like to acknowledge the State Key Development Program for Basic Research of China (No. 2009CB220004), the Science and Technology Commission of Shanghai Municipality (05nm05004), and the National High Technology Research and Development Program of China (No. 2009AA063003) for financial support. Thanks for support of FE-SEM lab in Instrumental Analysis Center of SJTU.

Appendix A. Supplementary data

Supplementary data associated with this article can be found, in the online version, at doi:10.1016/j.apcatb.2010.01.020.

References

[1] J.A. Turner, Science 285 (1999) 687–689.
[2] A. Fujishima, K. Honda, Nature 238 (1972) 37–38.
[3] D. Gong, C.A. Grimes, O.K. Varghese, W. Hu, R.S. Singh, Z. Chen, E.C. Dickey, J. Mater. Res. 16 (2001) 3331–3334.
[4] A. Ghicov, P. Schmuki, Chem. Commun. (2009) 2791–2808.
[5] J. Bai, B.X. Zhou, L.H. Li, Q. Zheng, Y.B. Liu, J.H. Shao, X.Y. Zhu, W.M. Cai, J. Mater. Sci. 43 (2008) 1880–1884.
[6] Q. Zheng, B.X. Zhou, J. Bai, L.H. Li, Z.J. Jin, J.L. Zhang, J.H. Li, Y.B. Liu, W.M. Cai, X.Y. Zhu, Adv. Mater. 20 (2008) 1044–1049.
[7] Y.B. Liu, B.X. Zhou, J.H. Li, X.J. Gan, J. Bai, W.M. Cai, Appl. Catal. B Environ. 92 (2009) 326–332.
[8] M. Paulose, K. Shankar, S. Yoriya, H.E. Prakasam, O.K. Varghese, G.K. Mor, T.A. Latempa, A. Fitzgerald, C.A. Grimes, J. Phys. Chem. B10 (2006) 16179–16184.
[9] O.K. Varghese, M. Paulose, K. Shankar, G.K. Mor, C.A. Grimes, J. Nanosci. Nanotechnol. 5 (2005) 1158–1165.
[10] S.U.M. Khan, M. Al-Shahry, W.B. Ingler, Science 297 (2002) 2243–2245.
[11] R. Asahi, T. Morikawa, T. Ohwaki, K. Aoki, Y. Taga, Science 293 (2001) 269–271.
[12] J.H. Park, S. Kim, A.J. Bard, Nano. Lett. 6 (2006) 24–28.
[13] R.S. Mane, M.Y. Yoon, H. Chung, S.H. Han, Sol. Energy 81 (2007) 290–293.
[14] J.S. Jang, H.G. Kim, P.H. Borse, J.S. Lee, Int. J. Hydrogen Energy 32 (2007) 4786–4791.
[15] G.K. Mor, O.K. Varghese, R.H.T. wilke, S. Sharma, K. Shankar, T.J. Latemap, K.S. Choi, C.A. Grimes, Nano. Lett. 8 (2008) 1906–1911.
[16] H. Zhu, B. Yang, J. Xu, Z. Fu, M. Wen, T. Guo, S. Fu, J. Zuo, S. Zhang, Appl. Catal. B Environ. 90 (2009) 463–469.
[17] S. Yamada, A.Y. Nosaka, Y. Nosaka, J. Electr. Chem. 585 (2005) 105–112.
[18] S. Chen, M. Paulose, C. Ruan, G.K. Mor, O.K. Varghese, D. Kouzoudis, C.A. Grimes, J. Photochem. Photobiol. A: Chem. 177 (2006) 177–184.
[19] Y. Yin, Z.G. Jin, F. Hou, Nanotechnology 18 (2007) 495608.
[20] C.L. Wang, L. Sun, H. Yun, J. Li, Y.K. Yue, C.J. Lin, Nanotechnology 20 (2009) 295601.
[21] C.L. Wang, S. Lan, K.P. Xie, C.J. Lin, Sci. Chin. Series B: Chem. (2009) 1–8.
[22] S. Banerjee, S.K. Mohapatra, P.P. Das, M. Misra, Chem. Mater. 20 (2008) 6784–6791.
[23] W.T. Sun, Y. Yu, H.Y. Pan, X.F. Gao, Q. Chen, L.M. Peng, J. Am. Chem. Soc. 130 (2008) 1124–1125.
[24] D.R. Baker, P.V. Kamat, Adv. Funct. Mater. 19 (2009) 805–811.
[25] C.J. Lin, Y.T. Lu, C.H. Hsieh, S.H. Chien, Appl. Phys. Lett. 94 (2009) 113102.
[26] X.W. Zhang, L.C. Lei, J.L. Zhang, Q.X. Chen, J.G. Bao, B. Fang, Sep. Purif. Technol. 66 (2009) 417–421.
[27] G. Larramona, C. Choné, A. Jacob, D. Sakakura, B. Delatouche, D. Péré, X. Cieren, M. Nagino, R. Bayón, Chem. Mater. 18 (2006) 1688–1696.
[28] S. Yoriya, M. Paulose, O.K. Varghese, G.K. Mor, C.A. Grimes, J. Phys. Chem. C 37 (2007) 13770–13776.
[29] G.K. Mor, O.K. Varghese, M. Paulose, K. Shankar, C.A. Grimes, Sol. Energy Mater. Sol. C 90 (2006) 2011–2075.
[30] J.L. Zhang, B.X. Zhou, Q. Zheng, J.H. Li, J. Bai, Y.B. Liu, W.M. Cai, Water Res. 43 (2009) 1986–1992.
[31] Y.B. Liu, J.H. Li, B.X. Zhou, J. Bai, Q. Zheng, J.L. Zhang, W.M. Cai, Environ. Chem. Lett. 7 (2009) 363–368.
[32] Y.B. Liu, B.X. Zhou, J. Bai, J.H. Li, J.L. Zhang, Q. Zheng, X.Y. Zhu, W.M. Cai, Appl. Catal. B Environ. 89 (2009) 142–148.
[33] D.S. Tsoukleris, I.M. Arabatzis, E. Chatzivasiloglou, A.I. Kontos, V. Belessi, M.C. Bernard, P. Falaras, Solar Energy 79 (2005) 422–430.
[34] J.H. Zhu, D. Yang, J.Q. Geng, D.M. Chen, Z.Y. Jiang, J. Nanopart. Res. 10 (2008) 729–736.